Dynamic Analysis of a Horizontal Oscillatory Cutting Brush

Libardo V. Vanegas-Useche[1, 4], Magd M. Abdel-Wahab[2, 3, *] and Graham A. Parker[5]

Abstract: Street sweeping is an important public service, as it has an impact on aesthetics and public health. Typically, sweeping vehicles have a gutter brush that sweeps the debris that lies in the road gutter. As most of the debris is located in the gutter, the effective operation of the gutter brush is important. The aim of this work is to study the performance of a type of gutter brush, the cutting brush, through a 3D dynamic (transient), large deflection finite element model developed by the authors. In this brush model, the brush mounting board is modelled as fixed, and, consequently, inertia forces are applied to the bristle, which is modelled as a beam element. In order to simulate the interaction with the road surface, this is rotated, translated, and raised. Bristle-road contact is modelled through a flexible-to-rigid contact pair. Particularly, the concept of a cutting brush rotating at variable speed is explored through the finite element analysis of a constrained horizontal cutting brush. This analysis helps to understand the behaviour of oscillatory cutting brushes for different frequencies of brush oscillation. It is concluded that, for a horizontal cutting brush, oscillations have an impact on bristle dynamics, and its performance may be improved by varying the brush rotational speed at certain frequencies.

Keywords: Gutter brush, cutting brush, FEA, variable speed, brushing.

1 Introduction

Street sweeping is an essential part of urban hygiene services and municipal solid waste management systems [Bartolozzi, Baldereschi, Daddi et al. (2018)]. In many countries, this service is provided by means of street sweepers. Despite its importance and the problems associated with it, research on street sweeping is rather limited, and it seems that most of the improvements have been achieved by sweeper manufacturers. Research has been focused mainly on pollution measurement and control, but also on dynamics of gutter brushes, sweeper automation, labour turnover, and route planning. A short review on this research is presented in a previous work [Vanegas-Useche and Parker (2004)].

[1] Facultad de Ingeniería Mecánica, Universidad Tecnológica de Pereira, La Julita, Pereira, 660003, Colombia.
[2] Division of Computational Mechanics, Ton Duc Thang University, Ho Chi Minh, Viet Nam.
[3] Faculty of Civil Engineering, Ton Duc Thang University, Ho Chi Minh, Viet Nam.
[4] Faculty of Engineering and Architecture, Ghent University, Soete Laboratory, Gent, Technologiepark Zwijnaarde 46 B-9052, Zwijnaarde, Belgium.
[5] Faculty of Engineering and Physical Sciences, The University of Surrey, Guildford, GU2 7XH, UK.
[*] Corresponding Author: Magd M. Abdel-Wahab. Email: magd.abdelwahab@tdtu.edu.vn.

Recent research has concentrated on pollution and environmental impact [Bartolozzi, Baldereschi, Daddi et al. (2018); Karanasiou, Moreno, Amato et al. (2012); Amato, Querol, Johansson et al. (2010); Keuken, Denier van der Gon and van der Valk (2010)], maintenance of permeable pavement surface [Winston, Al-Rubaei, Blecken et al. (2016)], and routing [Golden, Nossack, Pesch et al. (2017)].

Street sweepers usually have a gutter brush that sweeps the debris that is located in the road gutter. This brush plays an important role, as most of the debris on roads is located in the gutter [Peel (2002)]. Fig. 1 shows two commercial gutter brushes that have been used for testing: a cutting brush and a flicking brush, respectively.

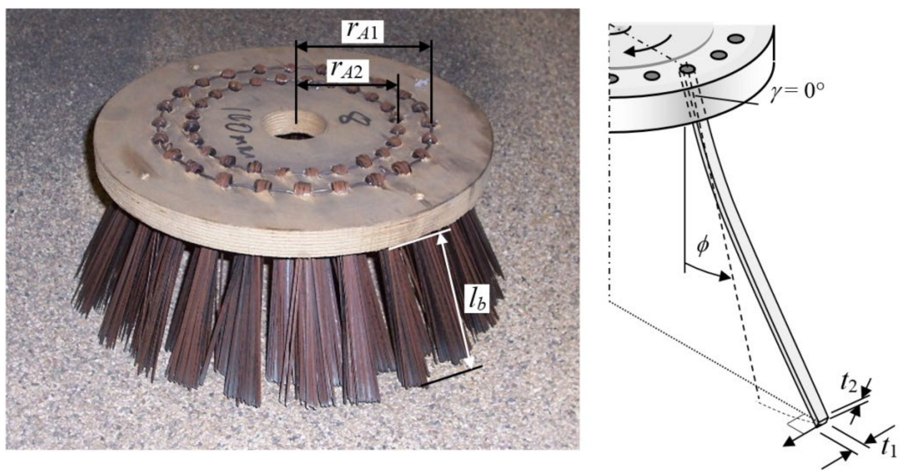

(a) Cutting brush

(b) F128 brush

Figure 1: Gutter brushes for road sweeping

These brushes have steel bristles of rectangular cross section and differ in their bristle mount orientation angles, γ. To be more precise, the flicking brush is called here the F128 brush, as the orientation of the bristles corresponds to a mount orientation angle of 128°

(this is measured relative to the mount orientation of the cutting brush), as shown in Fig. 1. In the cutting brush, the cross section is orientated in such a way that it provides a stiff collision, cutting through debris. In contrast, the bristles of the F128 brush may deflect easier and make more contact with the road surface.

In view of the importance of gutter brushes, research on them seems to have begun about two decades ago; however, not too much attention has been paid worldwide to gutter brushes. Firstly, Peel [Peel (2002)] and Peel et al. [Peel and Parker (2002)] developed analytical static models for cutting and flicking brushes, in order to gain an understanding of their characteristics. The models were validated by means of experimental tests, using a gantry test rig. Through these models brush vertical force, brush torque, and bristle deformation were determined. Later, improved models (static finite element models) were developed to study the dynamics and performance of gutter brushes [Wang (2005); Abdel-Wahab, Parker and Wang (2007); Abdel-Wahab, Wang, Vanegas-Useche et al. (2010)]. Besides, experimental tests were performed, in order to determine sweeping efficiency for different debris types [Vanegas-Useche, Abdel-Wahab and Parker (2010); Abdel-Wahab, Wang, Vanegas-Useche et al. (2011)]. In these tests, cutting brushes and F128 brushes were used. Also, a mathematical regression model [Wang, Sun, Abdel-Wahab et al. (2015)] was developed in order to be used in real time; this model was based on available Finite Element (FE) and experimental results. Finally, the novel concept of oscillatory brushes was studied, i.e., brushes that rotate at variable speed. Cutting and F128 brushes were studied by means of qualitative and quantitative experimental tests [Vanegas-Useche, Abdel-Wahab and Parker (2008b); Vanegas-Useche, Abdel-Wahab and Parker (2015b)] and analytical models [Vanegas-Useche, Abdel-Wahab and Parker (2007); Vanegas-Useche, Abdel-Wahab and Parker (2008a)]. In addition, the behaviour of horizontal F128 brushes was studied through FE analyses [Vanegas-Useche, Abdel-Wahab and Parker (2011a)].

Other brush types and brushing processes have also been the focus of research. However, the amount of literature is limited. The behaviour or performance of brushes for surface finishing operations has been studied by a few authors [Fitzpatrick and Paul (1987); Stango, Heinrich and Shia (1989); Shia, Stango and Heinrich (1989); Heinrich, Stango and Shia (1991); Stango, Cariapa, Prasad et al. (1991); Stango and Shia (1997)]. Research has also been conducted on surface fouling removal [Holm, Haslbeck and Horinek (2003)], air duct cleaning [Holopainen and Salonen (2002); Holopainen and Salonen (2004)], post-CMP (Chemical Mechanical Planarization) cleaning [Moumen and Busnaina (2001); Philipossian and Mustapha (2003); Huang, Guo, Lu et al. (2011); Sun, Zhuang, Li et al. (2012); Sun, Han and Keswani (2017)], and solar panel cleaning [Shehri, Parrott, Carrasco et al. (2016); Parrott, Carrasco Zanini, Shehri et al. (2018)].

Short literature reviews on sweeping and brushing may be found in previous works [e.g., Vanegas-Useche, Abdel-Wahab and Parker (2010); Vanegas-Useche, Abdel-Wahab and Parker (2015b); Vanegas-Useche, Abdel-Wahab and Parker (2011a); Vanegas-Useche, Abdel-Wahab and Parker (2006)].

This work applies the Finite Element Method (FEM), which is one of the best methods for solving engineering problems, such as structural, material science, and thermofluids problems [Zeng and Liu (2018)]. However, as the standard FEM has its limitations and drawbacks, alternative methods and variations, such as hybrid FEM and meshfree techniques, have been proposed to solve structural and engineering problems.

In particular, Smoothed Finite Element Methods (S-FEM) have recently been proven to be a valued combination of FEM with meshfree methods, addressing effectively many of the limitations of FEM by using some meshfree techniques; for example, S-FEM are more robust when dealing with huge deformations and mesh distortions and tend to exhibit higher accuracy and higher convergence rates in displacement [Zeng and Liu (2018)].

As an example of S-FEM developments, Nguyen-Xuan et al. [Nguyen-Xuan, Liu, Bordas et al. (2013)] develop an adaptive singular edge-based smoothed FEM (sES-FEM) for modelling mechanics problems with singular stress fields, such as crack propagation in a solid. They use a base mesh of triangles that can be generated automatically. A node is added on each edge of the triangular elements that are connected directly to the singular point. They conclude that the derived method is simple to implement into existing FE software. Also, the adaptive algorithm proposed exhibits high effectiveness. Similarly, Nguyen-Xuan et al. [Nguyen-Xuan, Nguyen-Hoang, Rabczuk et al. (2017)] propose a novel polytree-based adaptive FE scheme for the limit analysis of cracked bodies. A mesh refinement algorithm, based on a polytree mesh structure, is developed. The approach relies on a volumetric locking-free polygonal FE formulation. The work is focused on the plastic collapse of cracked bodies under plane-strain conditions. The results indicate that the method exhibits high accuracy at a low computational cost. Likewise, Chau et al. [Chau, Chau, Ngo et al. (2018)] propose a polytree-based adaptive mesh method for optimising multiphase material topology. In this approach, the polytree meshes, which are automatically refined based on error analysis, are used in conjunction with a novel definition of more efficient adaptive filters, in order to optimise results and clarify the interfaces between material phases. The boundaries obtained are smooth and the computational resources are reduced, when compared with a method that produces a fine mesh through the body.

In this work, the dynamic characteristics of horizontal (i.e., the brush mounting board is parallel to the road surface) oscillatory cutting brushes are studied by means of a FE model developed by Vanegas-Useche et al. [Vanegas-Useche, Abdel-Wahab and Parker (2011a)]; this model seems to be the only dynamic (transient) model that have been developed for gutter brushes. Similar to Vanegas-Useche et al. [Vanegas-Useche, Abdel-Wahab and Parker (2011a)], this paper considers a horizontal, constrained brush, i.e., a brush that is always in contact with the road surface, in order to evaluate the effects of the oscillations of the brush. However, the earlier paper studies an F128 brush, whereas this work investigates a cutting brush. Therefore, this work presents original results for a cutting brush; its novelty consists of determining the behaviour of an oscillatory cutting brush by means of FE modelling. As mentioned before, most of the debris on roadways is found in the gutter; thus, the efficient operation of gutter brushes is desired. In order to improve the effectiveness of gutter brushes, several studies referred to in the literature review have been carried out, and this work aims to investigate whether brush oscillations may improve sweeping effectiveness for a cutting brush and to determine an optimum frequency of oscillation.

2 Methodology

2.1 Brush geometry and configuration

The dynamic FE model developed may be used for different brush types and brushing processes. In this work, a cutting brush for street sweeping whose characteristics are given in Tab. 1 is studied. The bristle mount orientation angle (γ) was explained previously (see Fig. 1). Bristle length (l_b), bristle mount angle (ϕ), and mount radii (r_{A1} y r_{A2}) are illustrated in Fig. 1(a). The bristles of the gutter brush studied are of rectangular cross section, with a breadth t_1 and width t_2 (Fig. 1(a)) and are made of carbon steel. Brush angular speed (ω) varies according to the values in Tab. 1, i.e., it varies between 90 and 110 rpm. Vehicle speed (v) corresponds to the translational speed of the sweeping vehicle and, consequently, of the brush. Lastly, brush penetration (Δ) is the vertical distance the brush is lowered from first bristle contact. The values selected correspond to parameters that are typically used in the sweeping practice and that have been used in previous works.

Table 1: Gutter brush geometric and operating parameters and bristle material properties

Geometric and operating parameters and material properties	Symbol	Value
Number of bristles per cluster	n_{bc}	60
Number of clusters per row	n_c	24
Number of rows of clusters	n_r	1
Bristle mount angle	ϕ	27°
Bristle mount orientation angle	γ	0
Outer mount radius	r_{A1}	115 mm
Bristle length	l_b	240 mm
Bristle width	t_2	0.5 mm
Bristle breadth	t_1	2 mm
Mean brush rotational speed	ω_m	100 rpm
Alternating rotational speed	ω_a	10 rpm
Vehicle speed	v	1.5 m/s
Brush penetration	Δ	30 mm
Elastic modulus	E	207 GPa
Poisson ratio	ν	0.28
Density	ρ	7800 kg/m^3

2.2 Modelling assumptions and model description

This section describes the main characteristics of the FE model; a detailed description is provided in Vanegas-Useche et al. [Vanegas-Useche, Abdel-Wahab and Parker (2011a)].

The characteristics of a gutter brush are very complex, as there are many bristles of different lengths, usually they are not straight, they have different mount angles and mount orientation angles, and there are complex interactions among bristles, road, and debris. Therefore, it is necessary to use a simplified model of the brushing process. It is assumed that the bristles are rigidly clamped into the mounting board, the surface is flat and rigid, and there is no debris. Also, it is assumed that bristles of different clusters do not interact, because in a horizontal brush all the bristles tend to deform in a similar manner and to vibrate in phase; furthermore, because of the physical separation between adjacent clusters, there is less chance for the bristles of different clusters to interact. Also, as in a horizontal brush, whose bristle tips are always in contact with the road surface, there tends to be a low level of bristle-bristle interaction, it is suitable to model the brush by a single bristle for each row; its behaviour will represent the one of the whole cluster. These assumptions have been made in previous research [Peel (2002); Wang (2005); Abdel-Wahab, Parker and Wang (2007)]. The results of these works indicate that the assumptions made are practical.

The FE model is a parametric 3-D transient non-linear structural model developed in ANSYS®; it also involves contact modelling, which is highly non-linear. In gutter brushes, the bristles are subjected to large deformations, whereas road deformations are negligible. Therefore, the bristle is modelled with sixteen 3-D quadratic beams with 3 nodes (ANSYS® element BEAM189). The road surface is modelled through flat areas (no finite element is necessary, as the road is modelled as rigid). For the modelling of the interaction between the bristle tip and the road surface, the flexible contact element CONTA175 is attached to the bristle tip, and the rigid contact element TARGE170 is attached to the road areas. CONTA175 is a 2-D or 3-D node-to-surface contact element, and TARGE170 is the corresponding 3-D target element. The contact is modelled by means of the augmented Lagrangian method.

For modelling contact, there are some important parameters. The normal contact stiffness for bristle-surface interaction is taken as K_n=2 MN/m. This value has been determined in a previous work [Vanegas-Useche, Abdel-Wahab and Parker (2018)], based on the comparison between FE modelling and experimental results, for the interaction between a steel bristle and a concrete surface. Regarding bristle-surface friction, it is modelled by the exponential friction model:

$$\mu = \mu_k + (\mu_s - \mu_k) e^{-c_v |v_s|} \tag{1}$$

where μ is the coefficient of friction and μ_s and μ_k are the static and kinetic coefficients of friction, respectively. v_s is the relative sliding velocity and c_v is the decay coefficient. The values selected are μ_s = 0.70, μ_k = 0.27, and c_v = 0.40 s/m, which were determined by comparing experimental data with results of the developed FE model [Vanegas-Useche, Abdel-Wahab and Parker (2011b)]; these experiments were performed with horizontal brushes rotating at 60, 100, and 140 rpm.

Also, for the modelling of the damping produced by bristle internal friction, as well as bristle-bristle interaction within a cluster, Rayleigh damping is assumed. Based on experimental tests on clusters of gutter brushes, the values selected are: mass matrix multiplier for damping, α_D=3 s^{-1}, and stiffness matrix multiplier for damping, β_D=0.4 ms [Vanegas-Useche, Abdel-Wahab and Parker (2015a)].

The angular velocity, $\omega(t)$, and acceleration, $\alpha(t)$, functions, selected for studying the behaviour of the oscillatory cutting brush, correspond to the VAP function. This is a mathematical formulation that was developed by the authors to reduce the accelerations of the brush shaft [Vanegas-Useche, Abdel-Wahab and Parker (2007)]:

$$\omega(t) = \omega_m + \frac{2\omega_a h_2(t)}{1-b}\left[1 - b\, e^{(1/b-1)[2h_1(t)-1]}\right] \tag{2}$$

$$\alpha(t) = \frac{4 f \omega_a K_1}{1-b}\left\{1 - e^{(1/b-1)[2h_1(t)-1]} \times \left[b + 2(1-b)h_1(t)\right]\right\} \tag{3}$$

where ω_m and ω_a are the mean and alternating components of $\omega(t)$, f is the frequency of oscillation of $\omega(t)$, and

$$h_1(t) = \frac{1}{\pi}\arcsin\left(\sin\left\{\arccos\left[\cos\left(2\pi f t\right)\right]\right\}\right) \tag{4}$$

$$h_2(t) = \frac{1}{\pi}\left\{\arcsin\left[\sin\left(2\pi f t\right)\right]\right\} \tag{5}$$

$$K_1 = \begin{cases} 1, & \text{if } \mathrm{int}(2 f\, t + 0.5) \text{ is even} \\ -1, & \text{if } \mathrm{int}(2 f\, t + 0.5) \text{ is odd} \end{cases} \tag{6}$$

where the function “int” rounds the argument down to the nearest integer.

The key parameter of the VAP function is the *smoothness parameter b*. This can take any value in the interval (0, 1). Nevertheless, b should be close to 0 for minimising shaft accelerations; the value selected in this work is b=0.05.

Fig. 2 provides examples of the VAP function for $b\approx 0$ and b=0.1. When $b\approx 0$, $\omega(t)$ is a triangle wave and $\alpha(t)$ a square wave, so that the maximum angular acceleration of the brush is minimised; however, when $b\approx 0$, there are abrupt changes in the brush torque.

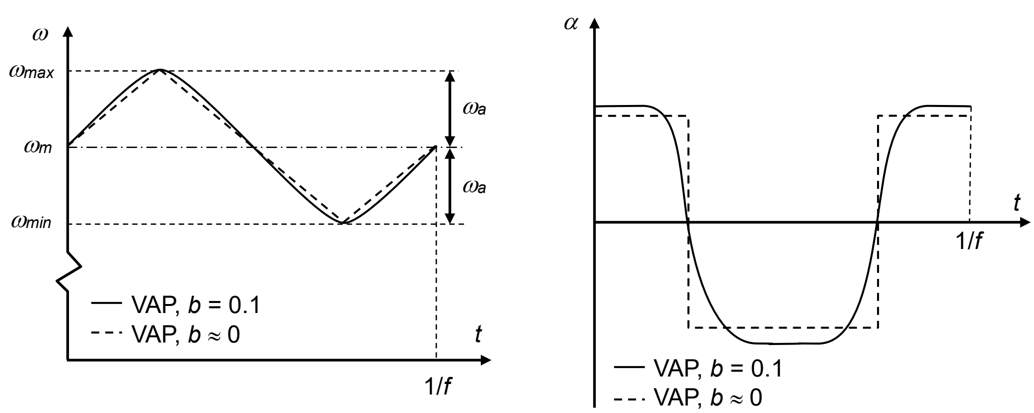

(a) Angular speed versus time (b) Angular acceleration versus time

Figure 2: VAP function

The FE model involves a dynamic (transient) analysis. In this model, the top of the bristle is totally constrained, and the rotation of the brush is modelled by means of inertia loads, whereas the surface is rotated, translated, and raised. As an example, Fig. 3 shows a simulation of the bristle for three time values. The bristle is subjected to gravity (g=9.8066 m/s^2) and centrifugal, tangential, and Coriolis forces. These loads are applied through the available ANSYS commands. Appropriate sensitivity analyses were performed. From their results, suitable values of the time step (i.e., the time used for applying loads and boundary conditions) is 0.1 ms, and of the integration time step (the time used for achieving convergence and the desired accuracy) is 5 μs [Vanegas-Useche, Abdel-Wahab and Parker (2018); Vanegas-Useche, Abdel-Wahab and Parker (2011a)].

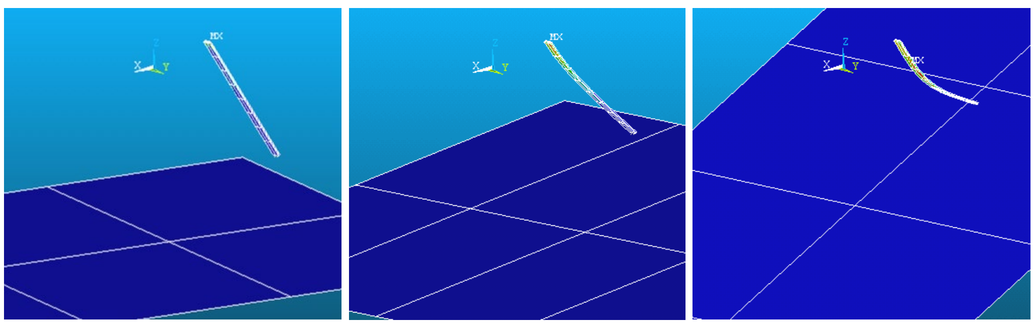

(a) t = 0 s (b) t = 0.125 s (c) t = 0.25 s

Figure 3: Example of the dynamic bristle model

In order to avoid a sudden application of the motion and inertia loads, there is an initial transitory stage. The brush is rotated from rest, at t=0, up to the nominal angular speed, at t=0.2 s. Brush penetration, Δ, is increased from Δ=0 up to its nominal value at t=0.6 s. From this time, Δ is held constant up to t=1.7 s. Numerous simulations were performed for both a brush rotating at constant speed and a brush oscillating from 1 Hz to 50 Hz. In order to study as many frequencies of speed oscillation as possible, brush oscillating frequency was varied progressively. For example, if f=7 Hz when t=0.7 s, f was increased each ω cycle up to about 8 Hz when t=1.7 s.

The useful time intervals for determining brush performance are [1.1 s, 1.32 s] and [1.575 s, 1.7 s]. These intervals were selected taking into account that, amongst other reasons: (a) in them the effects of the start-up of the brush are negligible, (b) the brush rotates about one revolution in the interval [1.1 s, 1.7 s], (c) the sweeping zone (i.e., the zone of the gutter that is in contact with the bristles of a tilted gutter brush) is the area of interest, and the bristle is outside of this area in about the interval [1.32 s, 1.575 s], (d) the speed of the bristle tip tends to be very small in this interval (because of the combination of bristle velocity relative to the mounting board and vehicle speed) and, consequently, the tip tends to stick to the road, and the sweeping action is reduced.

Fig. 4 shows a flowchart that provides the steps of the FE modelling. During solid modelling, entities such as points, lines, and areas are generated; these constitute the bristles and road surface. In the FE modelling, the finite elements for the bristle and the contact elements are created. Element types and properties are assigned, and the entities are meshed. Then, the analysis options are specified, the loads and boundary conditions are applied, and the solutions for the substeps are found. Finally, the postprocessing stage involves the revision and manipulation of the results given by the model.

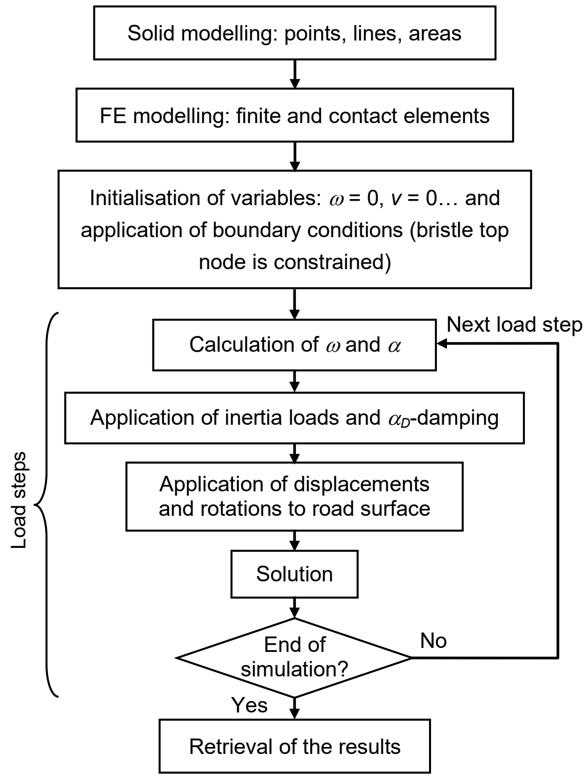

Figure 4: Flowchart of the dynamic brush model

Above, the main characteristics, assumptions, and parameters of the FE model were presented. A more detailed description is given in Vanegas-Useche et al. [Vanegas-Useche, Abdel-Wahab and Parker (2011a)], as mentioned previously.

Finally, the dynamics of the bristle is evaluated against some brushing performance criteria, which were defined in Vanegas-Useche et al. [Vanegas-Useche, Abdel-Wahab and Parker (2011a)] and are used to determine whether brush oscillations may improve performance. These criteria are based on debris removal mechanisms [Vanegas-Useche, Abdel-Wahab and Parker (2011a)]. Herein, a summarised description of the criteria is given.

It is assumed that for a given brush configuration [Vanegas-Useche, Abdel-Wahab and Parker (2011a)]:

(a) Effectiveness is higher when the *work of the road-bristle friction force*, W_{Ff}, is larger.

(b) Effectiveness is higher when the *maximum road-bristle friction force*, $F_{f\,max}$, is larger (a short-duration large friction force may dislodge compacted debris, and smaller forces may then be needed to remove the dislodged debris).

(c) Effectiveness is higher when the *"intensity" of the road-bristle friction force*, I_{Ff}, is greater. The parameter I_{Ff} is defined as the area under the friction force - bristle tip displacement curve, but above the line F_f=F_{fe}, where F_f is the magnitude of the road-bristle friction force and F_{fe} is the equivalent force that would produce the same work as the actual force. I_{Ff} is given by

$$I_{Ff} = \int_0^{\Delta s_{xy}} \left\langle F_f - F_{fe} \right\rangle \mathrm{d}s_{xy} \tag{7}$$

where s_{xy} is the position of the bristle tip, measured along its path on the plane of the surface, Δs_{xy} is the total distance travelled by the tip, and the function $\langle\ \rangle$ takes the value of the argument if this is positive and takes zero if it is negative. Fig. 5 illustrates the definition of I_{Ff}; this is represented by the shaded areas.

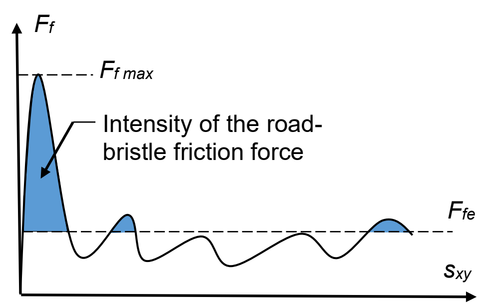

Figure 5: Definition of the intensity of the friction force

(d) Effectiveness is higher when the *area under the curve* v_{tip}^2-t is larger, where v_{tip} is the magnitude of the tip velocity and t is time. The square of the tip velocity is used, as the accelerations, forces, and kinetic energy that may be transferred to the debris tend to be proportional to it.

(e) Effectiveness increases with the *maximum value of* v_{tip}^2.

(f) Effectiveness is higher when $I_{v\,tip\hat{}2}$, the *"intensity" of* v_{tip}^2, is larger. A higher bristle tip velocity tends to enhance dislodging of compacted debris, and then smaller velocities may be needed to sweep the debris. Loosely speaking, the v_{tip}^2-t curve for the horizontal cutting brush studied in this work follows or fluctuates about a curve with a sinusoidal-squared shape (Fig. 6). Thus, $I_{v\,tip\hat{}2}$ is defined as the area under the curve v_{tip}^2-t, but above the curve $v_{tip(f=0)}^2$-t, where $v_{tip(f=0)}$ is the bristle tip velocity for a brush under the same conditions, excepting that the brush rotates at constant speed. The term $I_{v\,tip\hat{}2}$ is given by:

$$I_{vtip\hat{}2} = \int_0^{\Delta t} \left\langle v_{tip}^{\;2} - v_{tip(f=0)}^{\;\;2} \right\rangle \mathrm{d}t \tag{8}$$

Fig. 6 illustrates this concept; $I_{v\,tip\hat{}2}$ corresponds to the shaded areas.

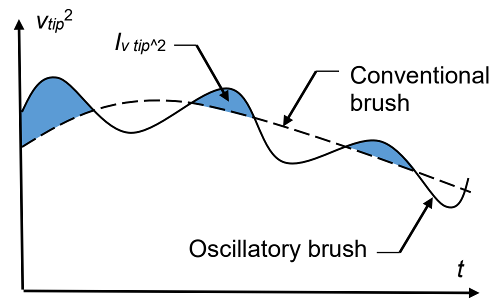

Figure 6: Definition of the intensity of v_{tip}^2

(g) Effectiveness is higher when the *direction of the velocity of the tip* exhibits high-frequency variability. This is because high frequency changes of the direction of v_{tip} may tend to sweep debris in different directions, which may improve debris removal. This criterion is quantified through the term ω_{vtipxy}, which is the rotational speed of v_{tip} on the plane of the surface. Taking into account that rotations of v_{tip} in any direction are assumed to be beneficial, absolute values are considered. Then, effectiveness tends to be higher when the average of the absolute values of ω_{vtipxy}, $\overline{|\omega_{v\,tip\,xy}|}$, is higher. However, when $v_{tip} = 0$, the value ω_{vtipxy} is taken equal to zero, as the tip will spin without sweeping.

All these criteria may be computed in some manner. Due to the complexities and all the phenomena involved in the sweeping process, an assessment of the relative performance of a cutting brush, based on the defined criteria, is not straightforward. In addition, the relative performance is strongly related to the type, amount, and conditions of the debris to be swept. Taking this into account, the proposed methodology for defining "a measure" of the performance is as follows.

The performance is a measure relative to a conventional brush; i.e., a conventional brush has 100% relative performance. For a given value of f, the relative performance, R_P, is the geometric mean of those for all the criteria:

$$R_P = R_{PW_{Ff}} \cdot R_{P\bar{v}_{tip}^2} \cdot R_{PI_{Ff}} \cdot R_{PI_{vtip\verb|^|2}} \cdot R_{PF_{f\max}} \cdot R_{Pv_{tip\max}^2} \cdot R_{P\overline{|\omega_{v\,tip\,xy}|}} \quad (9)$$

The individual relative performance values are given by the following equations:

$$R_{PW_{Ff}} = \frac{W_{Ff}}{W_{Ff(f=0)}} \quad \text{and} \quad R_{P\bar{v}_{tip}^2} = \frac{\bar{v}_{tip}^{\;2}}{\bar{v}_{tip(f=0)}^{\;2}} \quad (10)$$

$$R_{PI_{Ff}} = 1 + 0.3 \times \left(\frac{I_{Ff}}{I_{Ff(f=0)}} - 1 \right) \quad (11)$$

$$R_{PI_{vtip\verb|^|2}} = 1 + 0.3 \times \left(\frac{I_{vtip\verb|^|2}}{I_{vtip\verb|^|2(\max)}} \right) \quad (12)$$

$$R_{P\,F_{f\,\max}} = 1 + 0.1 \times \left(\frac{F_{f\,\max}}{F_{f\,\max(f=0)}} - 1 \right) \quad (13)$$

$$R_{P\,{v_{tip\,\max}}^2} = 1 + 0.1 \times \left(\frac{{v_{tip\,\max}}^2}{{v_{tip\,\max}}^2_{(f=0)}} - 1 \right) \quad (14)$$

$$R_{P\overline{|\omega_{v\,tip\,xy}|}} = 1 + 0.1 \times \left(\frac{\overline{|\omega_{v\,tip\,xy}|}}{\overline{|\omega_{v\,tip\,xy}|}_{(f=0)}} - 1 \right) \quad (15)$$

where the subscript "(f = 0)" indicates that the value referred to is for a conventional brush, and "(max)," in $I_{vtip\text{^}2(\max)}$, indicates that this corresponds to the maximum $I_{vtip\text{^}2}$ of all the frequencies studied.

The reasons for defining these equations are given herein. Regarding the work of the friction force, if, for example, W_{Ff}=0.0991 N m for a given frequency and $W_{Ff(f=0)}$=0.0947 N m, then $R_{P W_{Ff}}$ ≈1.05. This indicates that, for this criterion, the performance is 5% higher than that of a conventional brush. This is because the oscillatory brush does 5% more work than a conventional brush. The equation for the average squared tip velocity is similar, because this is related to the kinetic energy of the bristle.

Eqs. (11) to (15) are similar. For the intensity of the friction force, for instance, the equation has been defined so that a performance that is 30% higher than that of a conventional brush is assumed when I_{Ff}=2×$I_{Ff\,(f=0)}$, 60% when I_{Ff}=3×$I_{Ff\,(f=0)}$, etc. The equation for $I_{vtip\text{^}2}$ differs from the others, because the relative performance is taken with respect to the maximum value of $I_{vtip\text{^}2}$ for the range of frequencies studied. This is because the value for f=0 is zero, according to the definition of this variable. In addition, in Eqs. (13) to (15), 0.1 is taken instead of 0.3, because it is considered that the criteria related to these equations are less important.

It has to be noted that these equations have been defined based on analyses of experimental, analytical, and numerical results available for gutter brushes. However, they are preliminary guidelines that have the purpose of avoiding debris modelling; this would greatly increase the computing time. However, debris modelling is a natural extension to the model. Also, as brushing is a complex process, a more comprehensive assessment of sweeping efficiency would require advanced models.

3 Results and analysis

3.1 Main results

The main results of the analyses are shown in Figs. 7 to 9. From Figs. 7 and 9(a), it may be concluded that bristle kinematics is enhanced for a frequency of about 24 Hz to 25 Hz. For the force variables, the results appear to be more of a random nature than to follow certain trends (Fig. 8). This will be discussed in Section 3.3. According to Fig. 9(b), the maximum overall performance occurs for 24 Hz-25 Hz.

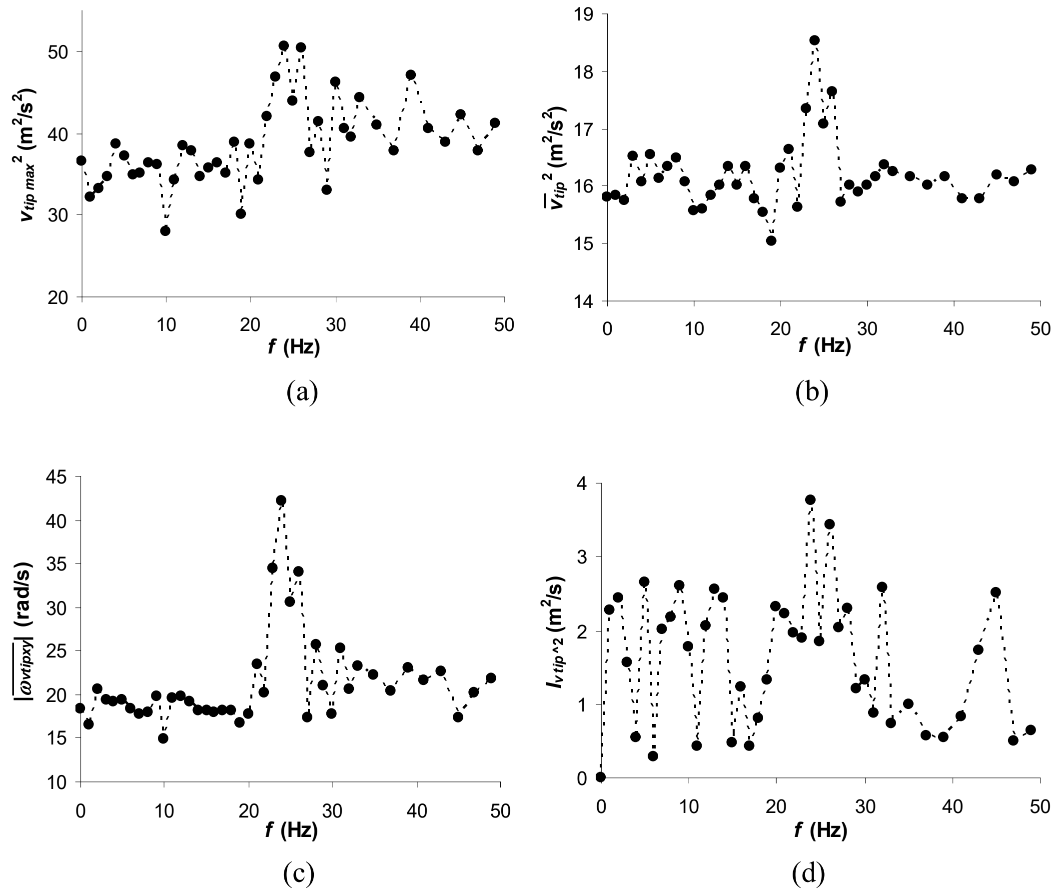

Figure 7: Kinematic variables against brush frequency

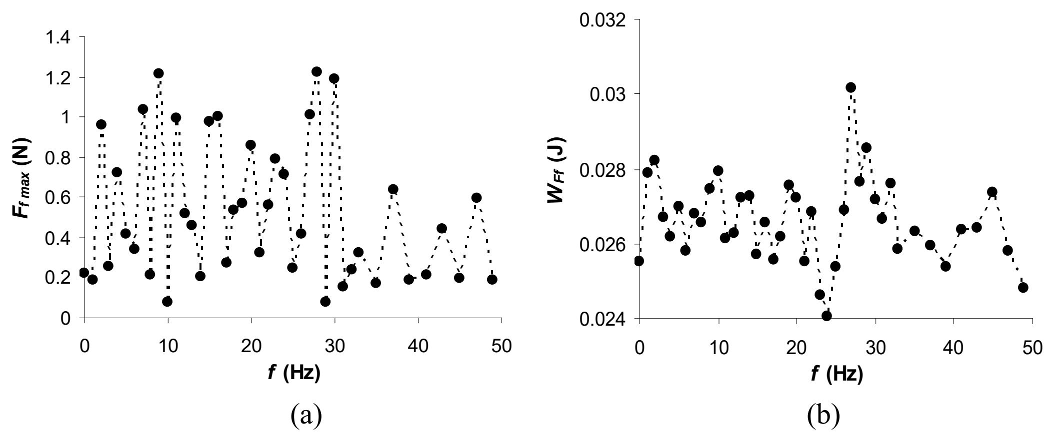

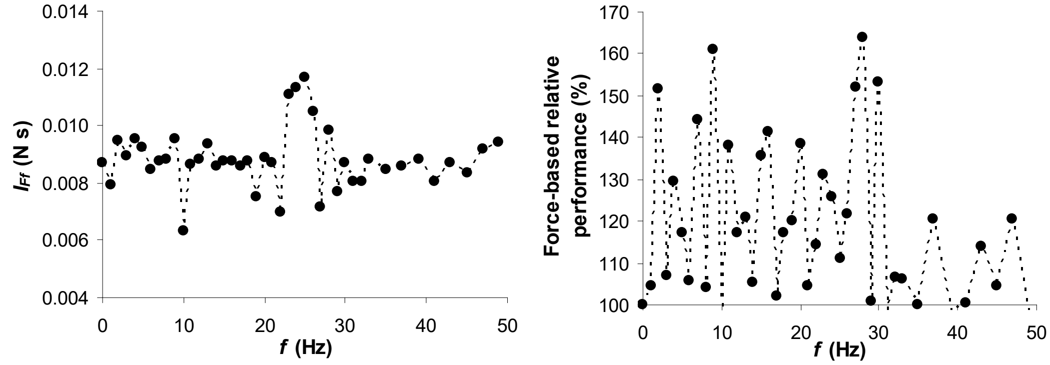

(c) (d)

Figure 8: Force-related variables against brush frequency

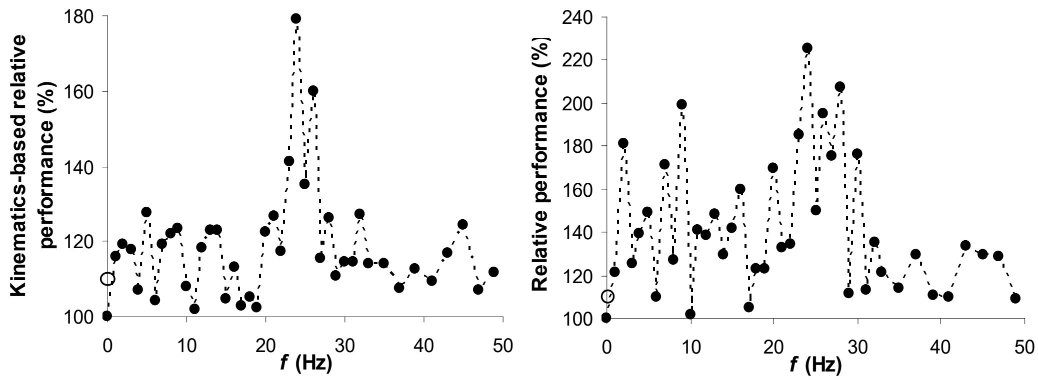

(a) Kinematics-based relative performance (b) Overall performance

Figure 9: Kinematics-based and overall relative performance

3.2 Motion and velocity of the bristle tip

An analysis of the results indicates that the path of the bristle tip, for most of the frequencies, seems quite smooth. However, for frequencies around 24 Hz, the tip tends to move with abrupt changes of direction. These issues are reflected in the examples given in Fig. 10, as well as Fig. 11, which shows curves $|\omega_{v\ tip\ xy}|$-t. This is in agreement with the results of the curves in Fig. 7. Therefore, a frequency close to 24 Hz seems to excite bristle vibrations.

Likewise, the curve v_{tip}^2-t exhibits the largest amplitudes of oscillation when f=24 Hz. To illustrate this, some examples are presented in Fig. 12. The results also indicate that the oscillations of this curve have a frequency of about 24 Hz, regardless of the frequency of oscillation of the brush. This is contrary to the case of the F128 brush [Vanegas-Useche, Abdel-Wahab and Parker (2011a)], whose curve v_{tip}^2-t presents oscillations whose frequency increases with the brush frequency, f.

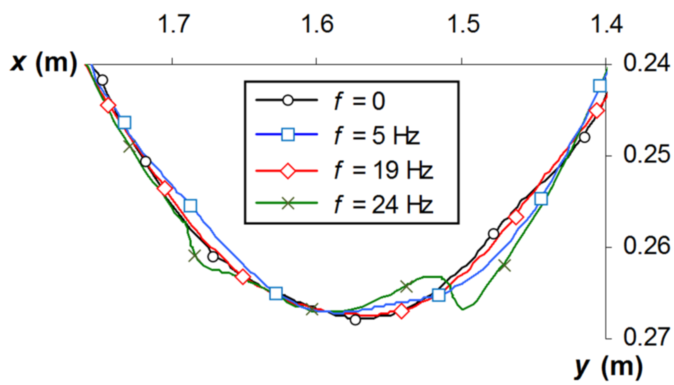

(a)

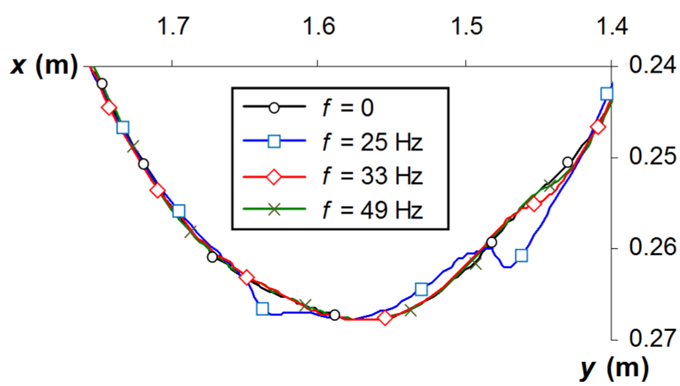

(b)

Figure 10: Path of the bristle tip, for a set of frequencies

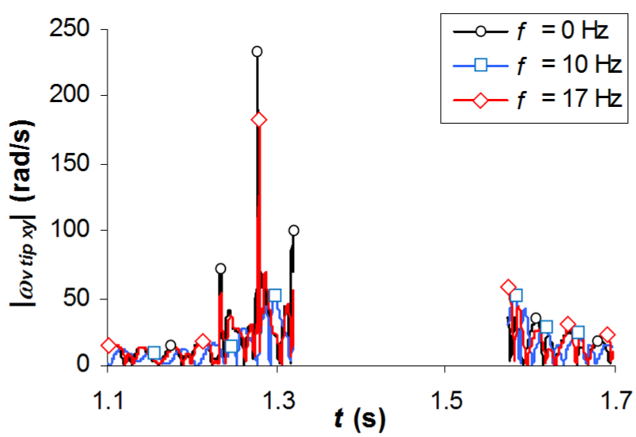

(a)

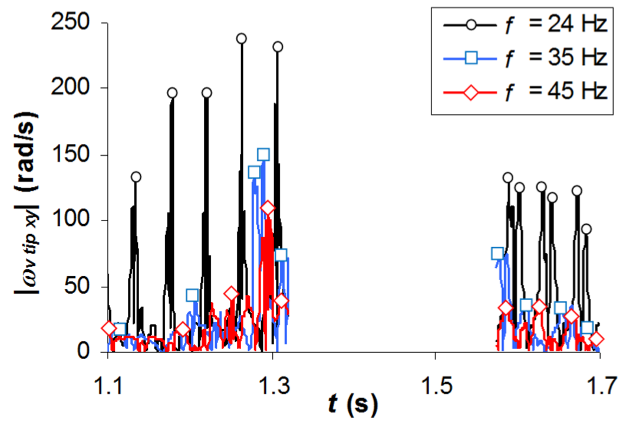

(b)

Figure 11: Absolute values of the angular speed of the tip velocity vector against time, for a set of frequencies

In fact, an analysis of the motion of the tip for the different frequencies reveals that as the tip slides on the surface, it exhibits oscillations. Relative to an observer fixed to the brush, it experiences small radial oscillations (in the weaker plane, i.e., the plane about which the moment of inertia of the cross section is smaller) and oscillations, much larger than the radial ones, in the direction of motion (in the stronger plane); the transverse oscillations cannot clearly be noticed in the tip path. Both oscillations present a frequency of about 24 Hz, regardless of the value of *f*. This is illustrated in Fig. 13. Due to the relatively small brush penetration (0.03 m), the oscillations cause that the tip separates and makes contact with the surface repeatedly. Consequently, when the brush oscillates at about 24 Hz, the oscillations of the tip are enhanced. It is also noted that, due to the tip oscillations in the transverse direction, the velocities of the tip are much higher than those of the F128 brush [Vanegas-Useche, Abdel-Wahab and Parker (2011a)], regardless of the value of *f*.

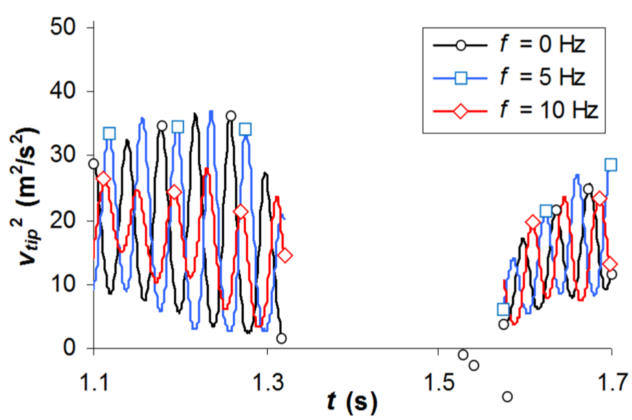

(a)

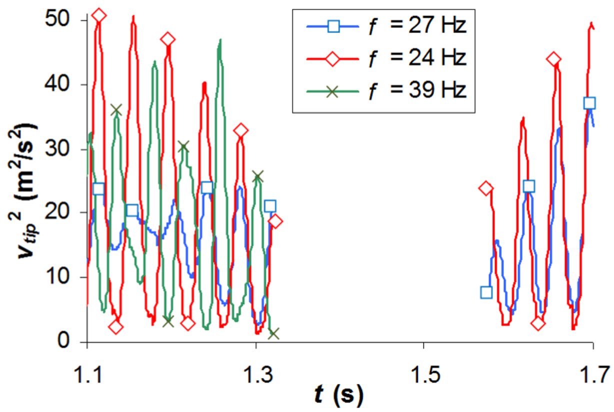

(b)

Figure 12: Tip velocity squared against time, for a set of frequencies

Finally, the curves in Fig. 12 suggest that not only are there brush frequencies that enhance bristle oscillations, but also there are frequencies, e.g., f=10 Hz, that hinder bristle oscillations or frequencies, e.g., f=5 Hz, that do not increase or decrease them significantly. Indeed, most of the frequencies do not affect significantly the average amplitudes of oscillation of the tip, as suggested by Figs. 7(b) and 7(c).

3.3 Friction forces

Fig. 14 shows examples of curves F_f-s_{xy} for a number of brush frequencies. It has to be noted that for some frequencies the friction forces reached are much higher than the maximum value of the scale in the figure (the maximum values of F_f are given in Fig. 8(a)). Contrary to the case of the F128 brush [Vanegas-Useche, Abdel-Wahab and Parker (2011a)], the curves tend to exhibit a similar pattern for most of the frequencies. The motion characteristics described in Section 3.2 are reflected in these curves. For instance, bristle tip oscillations cause variable tip velocities, which in turn produce a variable friction coefficient. These variations of μ, along with those of the normal force, produce the variations of the friction force. It may also be noticed that F_f=0 during some periods, i.e., tip-surface separation occurs, particularly as the bristle approaches the boundary zone (limit of the sweeping zone). These periods of separation are normally followed by high friction forces caused by the subsequent impact, as shown in Fig. 14. It is noted that the large bristle vibrations that occur for f=24 Hz produce more separation and impacts events than for most of the brush frequencies. Lastly, a comparison with the F128 brush [Vanegas-Useche, Abdel-Wahab and Parker (2011a)] shows that, due to the stiff collisions between a cutting bristle and the surface (motion is mainly in the direction of the stronger plane of the bristle), the friction forces are much higher than those for a F128 brush.

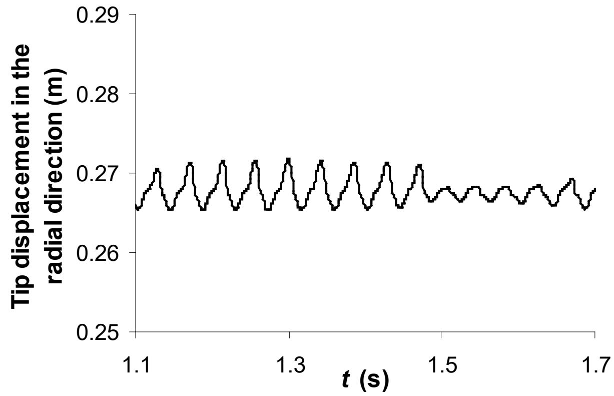

(a)

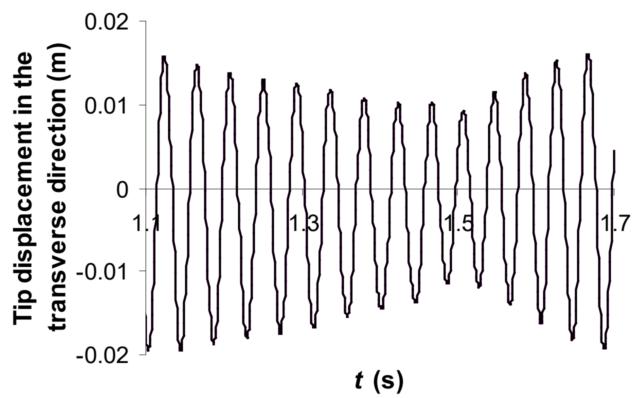

(b)

Figure 13: Radial and transverse displacement of the bristle tip with reference to the initial position; f=24 Hz

As mentioned in Section 3.1, there is not a clear tendency of F_{fmax}, W_{Ff}, and I_{Ff} with respect to f. Due to the stiff nature of the sweeping process in a cutting brush, high forces tend to be developed, even in a conventional brush. However, the results show that brush oscillations indeed tend to significantly increase bristle dynamics and contact forces. When f=24 Hz, resonance seems to occur. This may help in dislodging debris, due to the stiff collisions produced. However, the bristle tends to lose contact repeatedly, and this produces a small value of the work of the friction force (Fig. 8(b)). As when sweeping compacted debris higher penetrations may be required, this may remedy the separation problem. Also, frequencies close, but not equal, to 24 Hz may yield a higher performance. Finally, in a real sweeping scenario debris exists. This debris may change dramatically bristle dynamics in the case of a cutting brush due to the stiff nature of the sweeping process. Therefore, no definite conclusion may be reached in this case.

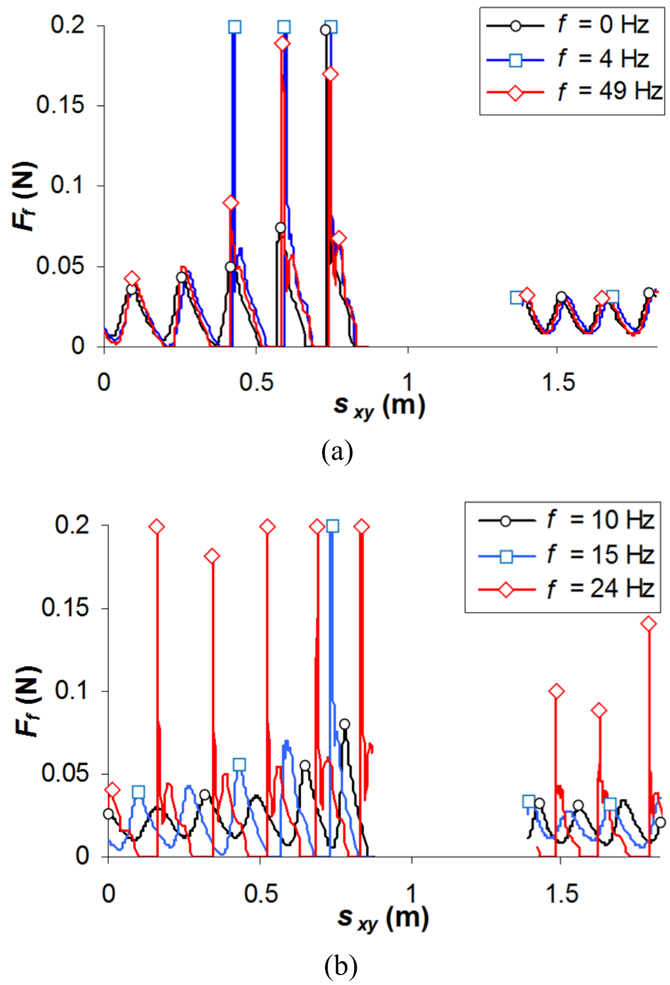

Figure 14: Friction force against *xy* tip displacement, for a set of frequencies

4 Conclusions

In this paper, a dynamic FE model was applied to study the behaviour and performance of an oscillatory horizontal cutting brush. This model is a generic, parametric model that may be applied to a variety of brushes for different brushing configurations. The brush is modelled with a single bristle, which is rigidly clamped into the brush mounting board. Brush rotation is simulated through inertia forces, and displacements and rotations are applied to the road surface. Bristle-surface interaction is modelled by means of contact pairs. The performance of the horizontal cutting brush was assessed against some performance criteria and using a measure of effectiveness.

It is concluded that brush oscillations, at certain frequencies, may be advantageous for the horizontal cutting brush. For instance, bristle kinematics (vibration) is enhanced for a frequency of about 24 Hz, and the maximum overall performance may be achieved with this frequency.

In previous works, experimental and analytical research on oscillatory gutter brushes was presented. It was found analytically [Vanegas-Useche, Abdel-Wahab and Parker (2008a)] that when the brush oscillates with the VAP function, enhanced oscillations may be achieved, for example, when the brush frequency is the first natural frequency of the bristle, but also when it is a third of this natural frequency. In the experimental research [Vanegas-Useche, Abdel-Wahab and Parker (2008b)], it was found that the cutting brush tends to exhibit enhanced bristle vibrations at 8 Hz, which is a third of 24 Hz, the frequency obtained in this work as an optimum one. The reason for not having obtained enhanced bristle vibrations at 24 Hz in the experimental research may be, amongst other factors, that the manner in which the oscillations were achieved was through a variable voltage in the motor. This variable voltage proved to be more effective for the lower frequencies, and at higher frequencies the voltage could not produce the desired shape and amplitude of the angular speed versus time curve, because of the inertia of the brush test rig. In conclusion, there is certain agreement between the FE results and the experimental results, but improved tests have to be carried out in order that the desired angular speed curve may be obtained, particularly at the higher frequencies. Lastly, future work may include new experimental tests, different brushing configurations, debris modelling, and a different assessment of sweeping performance.

Acknowledgements: The authors would like to acknowledge the support of the University of Surrey (UK), Ghent University (Belgium), Universidad Tecnológica de Pereira (Colombia), and the Programme Alβan, European Union Programme of High Level Scholarships for Latin America, identification number (E03D04976CO). The first author acknowledges the financial support provided by CWO (Commissie Wetenschappelijk Onderzoek), Faculty of Engineering and Architecture, Ghent University, for a visiting foreign researcher scholarship at Soete Laboratory.

References

Abdel-Wahab, M.; Parker, G.; Wang, C. (2007): Modelling rotary sweeping brushes and analyzing brush characteristic using finite element method. *Finite Elements in Analysis and Design*, vol. 43, no. 6-7, pp. 521-532.

Abdel-Wahab, M. M.; Wang, C.; Vanegas-Useche, L. V.; Parker, G. A. (2010): Finite element models for brush-debris interaction in road sweeping. *Acta Mechanica*, vol. 215, no. 1-4, pp. 71-84.

Abdel-Wahab, M. M.; Wang, C.; Vanegas-Useche, L. V.; Parker, G. A. (2011): Experimental determination of optimum gutter brush parameters and road sweeping criteria for different types of waste. *Waste Management*, vol. 31, pp. 1109-1120.

Amato, F.; Querol, X.; Johansson, C.; Nagl, C.; Alastuey, A. (2010): A review on the effectiveness of street sweeping, washing and dust suppressants as urban PM control methods. *Science of the Total Environment*, vol. 408, no. 16, pp. 3070-3084.

Bartolozzi, I.; Baldereschi, E.; Daddi, T.; Iraldo, F. (2018): The application of life cycle assessment (LCA) in municipal solid waste management: a comparative study on street sweeping services. *Journal of Cleaner Production*, vol. 182, pp. 455-465.

Chau, K. N.; Chau, K. N.; Ngo, T.; Hackl, K.; Nguyen-Xuan, H. (2018): A polytree-based adaptive polygonal finite element method for multi-material topology optimization. *Computer Methods in Applied Mechanics and Engineering*, vol. 332, pp. 712-739.

Fitzpatrick, P. R.; Paul, F. W. (1987): Robotic finishing using brushes-material removal mechanics. *Deburring and Surface Conditioning 87*, pp. 1-11.

Golden, B.; Nossack, J.; Pesch, E.; Zhanga, R. (2017): Routing problems with time dependencies or how different are trash collection or newspaper delivery from street sweeping or winter gritting? *Procedia Engineering*, vol. 182, pp. 235-240.

Heinrich, S. M.; Stango, R. J.; Shia, C. Y. (1991): Effect of workpart curvature on the stiffness properties of circular filamentary brushes. *Journal of Engineering for Industry*, vol. 113, no. 3, pp. 276-282.

Holm, E. R.; Haslbeck, E. G.; Horinek, A. A. (2003): Evaluation of brushes for removal of fouling from fouling-release surfaces, using a hydraulic cleaning device. *Biofouling*, vol. 19, no. 5, pp. 297-305.

Holopainen, R.; Salonen, E. M. (2002): Modelling the cleaning performance of rotating brush in duct cleaning. *Energy Buildings*, vol. 34, no. 8, pp. 845-852.

Holopainen, R.; Salonen, E. M. (2004): Rotating brush behaviour in duct cleaning. *Energy Buildings*, vol. 36, no. 10, pp. 1049-1062.

Huang, Y.; Guo, D.; Lu, X.; Luo, J. (2011): Modeling of particle removal processes in brush scrubber cleaning. *Wear*, vol. 273, no. 1, pp. 105-110.

Karanasiou, A.; Moreno, T.; Amato, F.; Tobías, A.; Boldo, E. et al. (2012): Variation of PM 2.5 concentrations in relation to street washing activities. *Atmospheric Environment*, vol. 54, pp. 465-469.

Keuken, M.; Denier van der Gon, H. D.; van der Valk, K. (2010): Non-exhaust emissions of PM and the efficiency of emission reduction by road sweeping and washing in the Netherlands. *Science of the Total Environment*, vol. 408, no. 20, pp. 4591-4599.

Moumen, N.; Busnaina, A. A. (2001): Removal of submicrometre alumina particles from silicon oxide substrates. *Surface Engineering*, vol. 17, no. 5, pp. 422-424.

Nguyen-Xuan, H.; Liu, G. R.; Bordas, S.; Natarajan, S.; Rabczuk, T. (2013): An adaptive singular ES-FEM for mechanics problems with singular field of arbitrary order. *Computer Methods in Applied Mechanics and Engineering*, vol. 253, pp. 252-273.

Nguyen-Xuan, H.; Nguyen-Hoang, S.; Rabczuk, T.; Hackl, K. (2017): A polytree-based adaptive approach to limit analysis of cracked structures. *Computer Methods in Applied Mechanics and Engineering*, vol. 313, pp. 1006-1039.

Parrott, B.; Carrasco Zanini, P.; Shehri, A.; Kotsovos, K. et al. (2018): Automated, robotic dry-cleaning of solar panels in Thuwal, Saudi Arabia using a silicone rubber brush. *Solar Energy*, vol. 171, pp. 526-533.

Peel, G. (2002): *A General Theory for Channel Brush Design for Street Sweeping (Ph.D. Thesis*). University of Surrey, UK.

Peel, G. M.; Parker, G. A. (2002): Initial investigations into the dynamics of cutting brushes for sweeping. *Journal of Dynamic Systems, Measurement, and Control*, vol. 124, no. 4, pp. 675-681.

Philipossian, A.; Mustapha, L. (2003): Effect of tool kinematics, brush pressure and cleaning fluid pH on coefficient of friction and tribology of post-CMP PVA brush scrubbing processes. *Materials Research Society Symposium*, vol. 767, pp. 209-215.

Shehri, A. A.; Parrott, B.; Carrasco, P.; Saiari, H. A.; Taie, I. (2016): Impact of dust deposition and brush-based dry cleaning on glass transmittance for PV modules applications. *Solar Energy*, vol. 135, pp. 317-324.

Shia, C. Y.; Stango, R. J.; Heinrich, S. M. (1989): Theoretical analysis of frictional effect on circular brush stiffness properties. *Deburring and Surface Conditioning 89*, pp. 1-18.

Stango, R. J.; Heinrich, S. M.; Shia, C. Y. (1989): Analysis of constrained filament deformation and stiffness properties of brushes. *Journal of Engineering for Industry*, vol. 111, no. 3, pp. 238-243.

Stango, R. J.; Cariapa, V.; Prasad, A.; Liang, S. K. (1991): Measurement and analysis of brushing tool performance characteristics, part 1: stiffness response. *Journal of Engineering for Industry*, vol. 113, no. 3, pp. 283-289.

Stango, R. J.; Shia, C. Y. (1997): Analysis of filament deformation for a freely rotating cup brush. *Journal of Manufacturing Science and Engineering*, vol. 119, no. 3, pp. 298-306.

Sun, T.; Han, Z.; Keswani, M. (2017): Chapter 4-Brush scrubbing for post-CMP cleaning. In: Rajiv Kohli and K. L. Mittal (eds.), *Developments in Surface Contamination and Cleaning: Methods for Surface Cleaning*, vol. 9, pp. 109-133.

Sun, T.; Zhuang, Y.; Li, W.; Philipossian, A. (2012): Investigation of eccentric PVA brush behaviors in post-Cu CMP cleaning. *Microelectronic Engineering*, vol. 100, pp. 20-24.

Vanegas-Useche, L. V.; Abdel-Wahab, M. M.; Parker, G. A. (2006): Brush dynamics: models and characteristics. *Proceedings of the 8th ASME Conference of Engineering Systems, Design, and Analysis ESDA*, pp. 441-450.

Vanegas-Useche, L. V.; Abdel-Wahab, M. M.; Parker, G. A. (2007): Dynamics of an unconstrained oscillatory flicking brush for road sweeping. *Journal of Sound and Vibration*, vol. 307, no. 3-5, pp. 778-801.

Vanegas-Useche, L. V.; Abdel-Wahab, M. M.; Parker, G. A. (2008a): Dynamics of a freely rotating cutting brush subjected to variable speed. *International Journal of Mechanical Sciences*, vol. 50, no. 4, pp. 804-816.

Vanegas-Useche, L. V.; Abdel-Wahab, M. M.; Parker, G. A. (2008b): Qualitative experimental behavior of oscillatory gutter brushes. *Proceedings of the 9th ASME Conference of Engineering Systems, Design, and Analysis ESD*, pp. 1-7.

Vanegas-Useche, L. V.; Abdel-Wahab, M. M.; Parker, G. A. (2010): Effectiveness of gutter brushes in removing street sweeping waste. *Waste Management*, vol. 30, no. 2, pp. 174-184.

Vanegas-Useche, L. V.; Abdel-Wahab, M. M.; Parker, G. A. (2011a): Dynamic finite element model of oscillatory brushes. *Finite Elements in Analysis and Design*, vol. 47, no. 7, pp. 771-783.

Vanegas-Useche, L. V.; Abdel-Wahab, M. M.; Parker, G. A. (2011b): Determination of friction coefficients, brush contact arcs, and brush penetrations for gutter brush-road interaction through FEM. *Acta Mechanica*, vol. 221, no. 1-2, pp. 119-132.

Vanegas-Useche, L. V.; Abdel-Wahab, M. M.; Parker, G. A. (2015a): Determination of the Rayleigh damping coefficients of steel bristles and clusters of bristles of gutter brushes. *Dyna*, vol. 82, no. 194, pp. 230-237.

Vanegas-Useche, L. V.; Abdel-Wahab, M. M.; Parker, G. A. (2015b): Effectiveness of oscillatory gutter brushes in removing street sweeping waste. *Waste Management*, vol. 43, no. 1, pp. 28-36.

Vanegas-Useche, L. V.; Abdel-Wahab, M. M.; Parker, G. A. (2018): Determination of the normal contact stiffness and integration time step for the finite element modeling of bristle-surface interaction. *Computers, Materials & Continua*, vol. 56, no. 1, pp. 169-184.

Vanegas-Useche, L. V.; Parker, G. A. (2004): Barrido de calles y vehículos barredores. *Scientia et Technica*, vol. 10, no. 26, pp. 85-90.

Wang, C. (2005): *Brush Modelling and Control Techniques for Automatic Debris Removal during Road Sweeping (Ph.D. Thesis)*. University of Surrey, UK.

Wang, C.; Sun, Q.; Abdel-Wahab, M.; Zhang, X.; Xu, L. (2015): Regression modeling and prediction of road sweeping brush load characteristics from finite element analysis and experimental results. *Waste Management*, vol. 43, pp. 19-27.

Winston, R.; Al-Rubaei, A. M.; Blecken, G. T.; Viklander, M.; Hunt, W. F. (2016): Maintenance measures for preservation and recovery of permeable pavement surface infiltration rate-The effects of street sweeping, vacuum cleaning, high pressure washing, and milling. *Journal of Environmental Management*, vol. 169, pp. 132-144.

Zeng, W.; Liu, G. R. (2018): Smoothed Finite Element Methods (S-FEM): an overview and recent developments. *Archives of Computational Methods in Engineering*, vol. 25, pp. 397-435.